Journal of Applied Polymer Science

Nickel-Multiwalled Carbon Nanotubes/Polyvinylidene Fluoride Composites with High Dielectric Permittivity

Dan-dan Yang, Hai-ping Xu, Jing-rong Wang, Yi-hua Wu
School of Urban Development and Environmental Engineering, Shanghai Second Polytechnic University, Shanghai 201209, People's Republic of China
Correspondence to: H.-P. Xu (E-mail: hpxu@sspu.edu.cn)

ABSTRACT: Composites with nickel particles coated multiwalled carbon nanotubes (Ni-MWNTs) embedded into polyvinylidene fluoride (PVDF) were prepared by solution blending and hot-press processing. The morphology, structure, crystallization behavior, and dielectric properties of composites were studied. The results showed that the crystallization of PVDF was affected by Ni-MWNTs. With the increment of Ni-MWNTs, the content of β-phase in PVDF increased. The dielectric permittivity was as high as 290 at 10^3 Hz when the weight fraction of Ni-MWNTs was 10%. The results can be explained by the space charge polarization at the interfaces between the insulator and the conductor, and the formation of microcapacitance structure. © 2013 Wiley Periodicals, Inc. J. Appl. Polym. Sci. 130: 3746–3752, 2013

KEYWORDS: composites; dielectric permittivity; nickel-multiwalled carbon nanotubes; nanotubes; properties and characterization

Received 23 March 2013; accepted 8 June 2013; Published online 29 June 2013
DOI: 10.1002/app.39645

INTRODUCTION

Dielectric composite materials of polymer matrix with inorganic or organic fillers have been studied because of inimitable electric properties and potential applications in many fields, such as embedded capacitors, artificial muscles, and electric energy storage devices.[1–4] Frequently, semicrystalline polyvinylidene fluoride (PVDF) has been selected as the polymer host because the PVDF-based composite materials have already been commercialized in pyroelectric, piezoelectric, and some actuator applications.[5–7] Therefore, many researchers have paid attention to dielectric properties of PVDF-based composites in recently years. For such applications, it has been necessary to enhance dielectric permittivity of PVDF-based composites.[8–10] Traditional approach of obtaining the high-dielectric-permittivity of PVDF-based composites is to add high-dielectric-permittivity ceramic powder into the PVDF matrix randomly.[11–13] However, the applications of such composites are seriously limited because of their disadvantages such as flexibility loss and incompatibility, giving rise to the focus on the metal particles or carbon nanotubes (CNTs) filled PVDF composites.[14–17] Especially, PVDF composites filled by CNTs possess a high dielectric permittivity at a low filler concentration and thus make it possible to preserve the flexibility of the polymer matrix.

CNTs is suitable to be conductive fillers in a polymer matrix and gives rise to very low percolation thresholds because of their high electrical and thermal conductivity values, high slenderness ratios and low molecular weights. Polymer composites exhibit a low percolation threshold and CNTs have excellent mechanical strength, which contribute to achieving flexibility and desired elastic modulus values of composites. Recently, it has been found that the dielectric properties of CNTs/polymer composites have differed depending on the pre-treatment of conductive fillers and method of preparation for composites to a large extent.[6,7,18]

In this study, we report a (Ni-MWNTs)/PVDF composite with high dielectric permittivity at low percolation threshold. PVDF is selected as the polymer matrix because of its dielectric performance and one goal of this study is to investigate whether this property can be retained or enhanced in composite of PVDF with nickel coated MWNTs. Dielectric property of PVDF is associated with its β crystalline form, and among many ways to enhance the formation of β phase, such as crystallization from solution, through orientation by applying forces at 80–100°C, the addition of metal particles or CNTs into the PVDF matrix.[14,16,19,20] Thus this research employs the chemical functionalized MWNTs as conductive fillers, which is coated by nickel particles via electroless plating. Our previous work reported a Ni/PVDF composite with a dielectric permittivity of about 90 at 10^2 Hz. However the volume fraction of nickel particles was required no less than 0.20, which

Additional Supporting Information may be found in the online version of this article.

Table I. Chemical and Concentration for Electroless Plating of MWNTs with Nickel

Chemical	Concentration (g/L)
$NiSO_4{\cdot}6H_2O$	25
$NaH_2PO_2{\cdot}2H_2O$	15
$NaHC_6H_5O_7{\cdot}1.5H_2O$	5
NH_4Cl	60

subjected composites to several inevitable limitations, such as low flexibility and hard processing because of the serious agglomeration of nickel particles.[14] On the other hand, because of the intensive van der Waals interaction between nanotubes, CNTs usually tend to aggregate.[21] The chemical functionalized MWNTs are activated to be better dispersed in polymer matrix. Moreover, MWNTs coated by nickel particles have magnetic so that it trends to form parallel capacitor structure in host polymer in external magnetic field, which is conducive to obtain composite with high dielectric permittivity. X-ray diffractometry (XRD), Fourier transform infrared spectroscopy (FTIR), and differential scanning calorimetry (DSC) measurements confirmed the presence of β phase in (Ni-MWNTs)/PVDF composites. The morphology of the composites was obtained by scanning electron microscopy (SEM). The micrographs show that the Ni-MWNTs are well dispersed and form some parallel structure in PVDF matrix. The dielectric permittivity was as high as 290 at 10^3 Hz when the weight fraction of Ni-MWNTs was 10%.

EXPERIMENTAL

Materials and Experimental Procedures

The MWNTs were provided by Shenzhen Nanotech Port Co., Ltd with the average length of 5 μm and the diameter of 30–50 nm. The Ni-MWNTs with the average length of about 5 μm and the diameter of 50–100 nm were prepared according to the method of Kong et al.[22] Chemicals of the electroless plating solution in this experiment were all A.R. and purchased from Sinopharm Chemical Reagent Co. Ltd, China. MWNTs were immersed into an aqueous solution (0.1 M of $SnCl_2$/0.1 M of HCl) and stirred at room temperature for 0.5 h, followed by filtering and washing with deionized water. The sensitized MWNTs were vigorously refluxed in an aqueous mixture of 0.0014 M of $PdCl_2$ and 0.25 M of HCl for activation at room temperature for another 0.5 h. After washing, activated MWNTs were put into plating solution. Chemicals and their concentrations of the plating solution were shown in Table I. Ammonia solution was employed as buffer to adjust and maintain pH value. The electroless plating was carried at room temperature for 20 min with agitation. Samples after electroless plating were characterized with SEM [as shown in Figure 1(b)] and XRD (see the Supporting Information Figure S1). Figure 1(a) shows the tubular morphology of the uncoated MWNTs with a diameter of 30–50 nm. From Figure 1(b) one can see that the Ni-coated MWNTs show a typical granular surface morphology. Compared to the uncoated MWNTs, the Ni-MWNTs are thicker (50–100 nm diameter) and their external surface is not smooth.

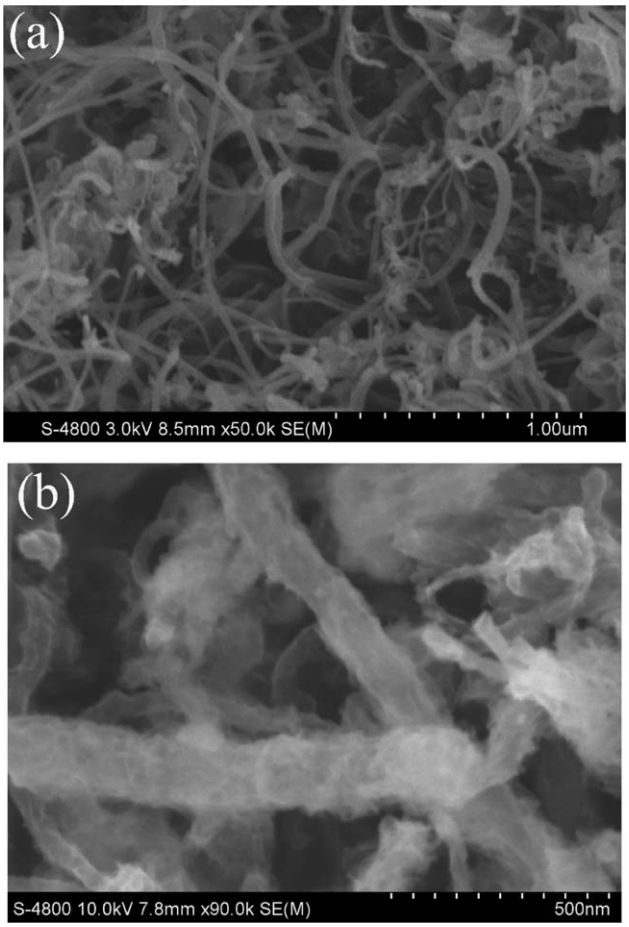

Figure 1. SEM images of (a) unpurified MWNTs and (b) Ni-coated MWNTs.

The semicrystalline polymer PVDF (FR903, the melt index is 2.0 g/10 min) powder was supplied by Shanghai 3F New Materials Ltd. *N*,*N*-dimethylformamide (DMF) was purchased from Sinopharm Chemical Reagent Co. Ltd, China. The (Ni-MWNTs)/PVDF composites were prepared by a solution method. All ultrasonic treatments were carried out in the ultrasonic equipment (SK1200H, Shanghai Kudos. Ultrasonic Instrument Co. Ltd., 59 kHz). The PVDF was first dissolved in DMF. Ni-MWNTs were dispersed in DMF by bath-sonicating for 50 min. Then, the suspension of Ni-MWNTs in DMF was added into PVDF solution. The mixture solution was stirred by ultrasonic treatment for 50 min and further magnetic stirring for 4 h. After the mixture solution was placed in a magnetic field of 0.2 T to be stand for 1 h, the mixture solution was dried at 85°C in oven for 24 h and then molded by hot pressing at about 200°C and 18 MPa for 20 min and slowly cooled to room temperature under the pressure. The final samples with a disk shape were 12 mm in diameter and around 1 mm in thickness. For electrical measurement, electrodes were painted with silver paste. A series of (Ni-MWNTs)/PVDF composites with a wide range of Ni-MWNTs contents of 0–12 wt % were fabricated.

Characterization

XRD patterns of the as-prepared samples were obtained using nickel-filtered Cu-Kα radiation (XRD, Bruker D8-Advance, Germany). The FTIR spectra of these samples were then measured (FTIR, Bruker V-70, Germany). The thermal analysis of composites was studied by DSC (DSC, STA-449C, Germany), and the samples were heated to 220°C at a rate of 10°C/min. Microstructures of fractured surfaces of composites were observed by SEM (SEM, HITACHI S-4800, Japan). The samples were gold sputtered in vacuum prior to observation. The dielectric properties of all the samples were measured by Novocontrol TOP Class Dielectric Spectrometer with an Alpha-A high performance analyzer (DBS-80, Germany) in frequency ranges of 10^3-10^7 Hz. The working electrodes with diameter of 12 mm and thickness of 0.05 mm were prepared by painting silver paste on both sides of the samples.

RESULTS AND DISCUSSION

As well known, there are mainly five crystalline phases with different conformations in PVDF, and they are designated as TGTG′ for the α- and δ-phases, all trans (TTT) planar zigzag for the β-phase, and T_3GT_3G' for the γ- and ε-phases.[23,24] Among them, the β-phase has the largest spontaneous polarization per unit cell and the γ-phase ranks second, thus providing the piezoelectric properties.[25] A lot of research indicated that the addition of the nanofillers will induce the β-phase PVDF.[26,27] It can be seen that the addition of Ni-MWNTs indeed induced the β-phase PVDF. The reason is believed to be the fact that MWNTs surface has zigzag carbon atoms and those atoms match with the all-trans conformation of β-phase PVDF, and as a result induce crystallization of PVDF in the β polymorphic structure.[28] However, other nanofiller with different form, such as metal particles, can induce β-phase PVDF too. So the nature of the nanofiller-inducing β polymorphic structure is not completely clear yet.

Structure and Crystallization Behavior of the Composites

XRD presents the direct characterization of the PVDF crystal forms. Figure 2 presents the XRD results of the pure PVDF and (Ni-MWNTs)/PVDF composites. Three characteristic diffraction peaks are observed at 17.7°, 18.4°, and 19.9° for pure PVDF, which are assigned to (100), (020), and (110) reflections of α-phase crystal,[29] indicating that the dominant phase is the α-phase in the pure PVDF. The characteristic diffraction peak of the β-phase is 20.5° (200, 110) and 20.3° (101) is assigned to the γ-phase.[30] When Ni-MWNTs is added, a broad double peak appears around 20.4°, the peak can be ascribed to the γ-phase and the β-phase, but the two peaks are hard to distinguish from each other. This means that incorporation of Ni-MWNTs induces formation of the polar phases. Really the broad double peak at 20.4° can be also observed in XRD pattern of pure polymer [see the Figure 2(a)], nevertheless, the relative intensity of this peak for pure polymer is much weaker than that for the (Ni-MWNTs)/PVDF composites. Hence, nonpolar α-phase is supposed to be the dominant phase in the pure PVDF. The relative intensity of the characteristic polar peaks at 20.4° is stronger for the (Ni-MWNTs)/PVDF samples with 2 wt % [as shown in Figure 2(b)] and 4 wt % [as shown in Figure 2(d)] Ni-MWNTs

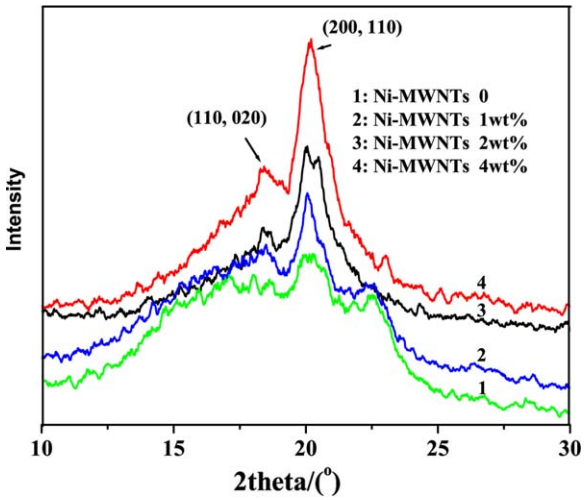

Figure 2. XRD pattern of pure PVDF and (Ni-MWNTs)/PVDF composites, in which Ni-MWNTs content is 0, 1, 2, and 4 wt %, respectively. [Color figure can be viewed in the online issue, which is available at wileyonlinelibrary.com.]

compared to that for the (Ni-MWNTs)/PVDF sample with 1 wt % [as shown in Figure 2(b)] Ni-MWNTs because the increased polar crystal forms when additions of Ni-MWNTs is increased.

This result can be further confirmed by FTIR, as shown in Figure 3. It is well known that the absorptions of the α-phase in PVDF are 763, 795, 855, and 978 cm^{-1}; of the β-phase are 445, 510, 840, 878, and 1403 cm^{-1}; and of the γ-phase are 430, 510, 811, and 1233 cm^{-1}.[31–33] For the (Ni-MWNTs)/PVDF composites, the dominant phase is the β-phase, which show peaks at 445, 510, 840, 878, and 1403 cm^{-1} in Figure 3. However, very weak peaks at 430 and 811 cm^{-1} can also be observed, which means that trace amounts of polar γ-phase are also present in (Ni-MWNTs)/PVDF composites. Simultaneously the peak intensities at 978 and 763 cm^{-1} start to diminish from 1 wt % loadings of Ni-MWNTs and almost disappear at 2 and 4 wt % loadings of Ni-MWNTs. From the XRD and FTIR results it can be concluded that Ni-MWNTs act as a nucleation agent for polar phase formation and its enhancement in PVDF, therefore, the PVDF composites acquired piezoelectric properties.

The nucleation effect of Ni-MWNTs is confirmed by differential scanning calorimetry (DSC) study as well. It has been reported that the melting temperature of the α-phase is lower than that of the polar β- and γ-phases for PVDF.[34,35] As a result, the rate of crystallization of the polymer increases, and in most cases the melting temperature also increases. Figure 4 illustrates the DSC heating curves of pure PVDF and (Ni-MWNTs)/PVDF composites. It is apparent from Figure 4 that the pure PVDF exhibits a melting peak at about 164.4°C. The (Ni-MWNTs)/PVDF composites contains more polar (β and γ forms) crystals that melt at higher temperature. For the (Ni-MWNTs)/PVDF samples with 1, 2, and 4 wt % Ni-MWNTs, the melting peak at 164.8°C, 165.6°C, and 167.2°C can be observed, respectively, suggesting that the sample is becoming a polar phase with higher melting temperature, in agreement with XRD and FTIR results. This

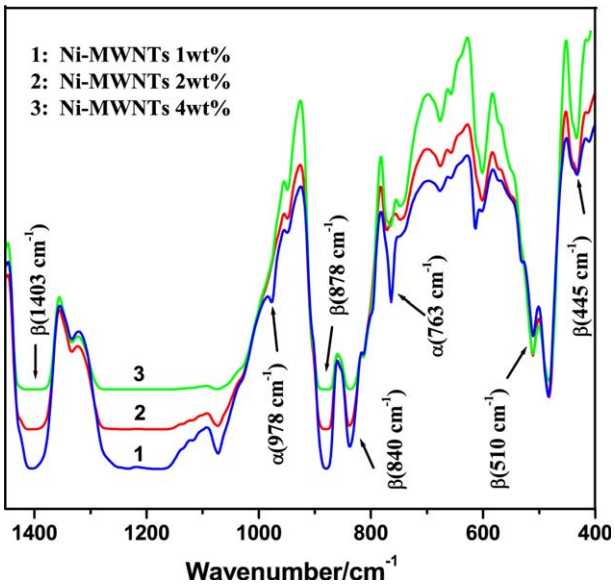

Figure 3. FTIR spectra of (Ni-MWNTs)/PVDF composites, in which Ni-MWNTs content is 1, 2, and 4 wt %, respectively. [Color figure can be viewed in the online issue, which is available at wileyonlinelibrary.com.]

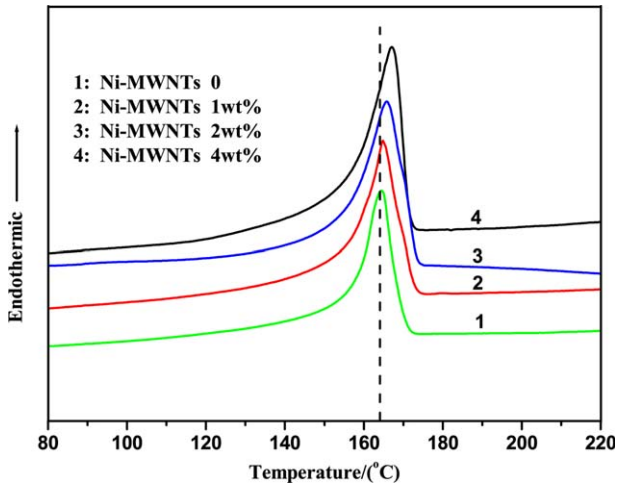

Figure 4. DSC curves of pure PVDF and (Ni-MWNTs)/PVDF composites, in which Ni-MWNTs content is 0, 1, 2, and 4 wt %, respectively. [Color figure can be viewed in the online issue, which is available at wileyonlinelibrary.com.]

means that the Ni-MWNTs take the role as the nucleation agent for PVDF and accelerate crystallization of PVDF.

Dispersion of Ni-MWNTs in PVDF Matrix

Figure 5 shows the typical SEM images of the composites with 4 wt % Ni-MWNTs. It can be seen that the Ni-MWNTs are almost homogeneously dispersed in the PVDF matrix, as shown in Figure 5(a). From Figure 5(b) one can observe that Ni-MWNTs are entrapped into polymer matrix and paralleled along the black arrow. For traditional melt processing, it is very hard to achieve such good dispersion at this Ni-MWNTs concentration. Three factors are believed to contribute to the good dispersion of Ni-MWNTs in the PVDF matrix. First, it is known that the solution blending method is an easy way to achieve good dispersion, especially with ultrasonic treatment and magnetic stirring. Second, the chemical treatment of electroless-activated MWNTs helped the dispersion of Ni-MWNTs in the solvent and hence formed a stable suspension. Third, external magnetic field may arrange Ni-MWNTs in parallel orientation to avoid agglomeration in the process of evaporation of the solvent, as shown in Figure 5(b). However, the completely homogeneous dispersion of Ni-MWNTs at higher concentration, such as 10 wt % is hard to achieve in a whole polymer matrix. In this case, good dispersion of filler may be realized in part areas of matrix.

Dielectric Properties of the Composites

Figure 6(a) shows the electrical conductivity of the pure PVDF and (Ni-MWNTs)/PVDF composites with various Ni-MWNTs contents as a function of electric field frequency of 10^3-10^7 Hz. It is found that electrical conductivity of the composites is strongly dependent on the applied electric field frequency as well as the Ni-MWNTs content. For the pure PVDF and composites with low Ni-MWNTs contents of 2 wt %, electrical conductivity is $\sim10^{-10}$ S/cm at 10^3 Hz and it increased with the increment of the frequency. This low electrical conductivity as well as its increasing trend with the electric field frequency demonstrates that the pure PVDF and composites with low Ni-

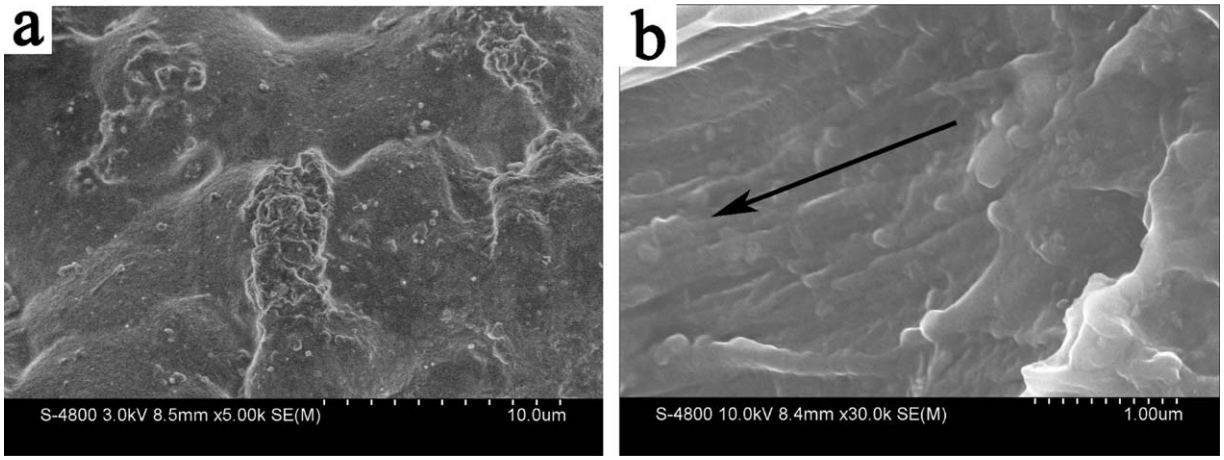

Figure 5. SEM images of (a) surface morphology and (b) freeze-fractured surface morphology of composite with 4 wt % Ni-MWNTs.

Applied Polymer SCIENCE

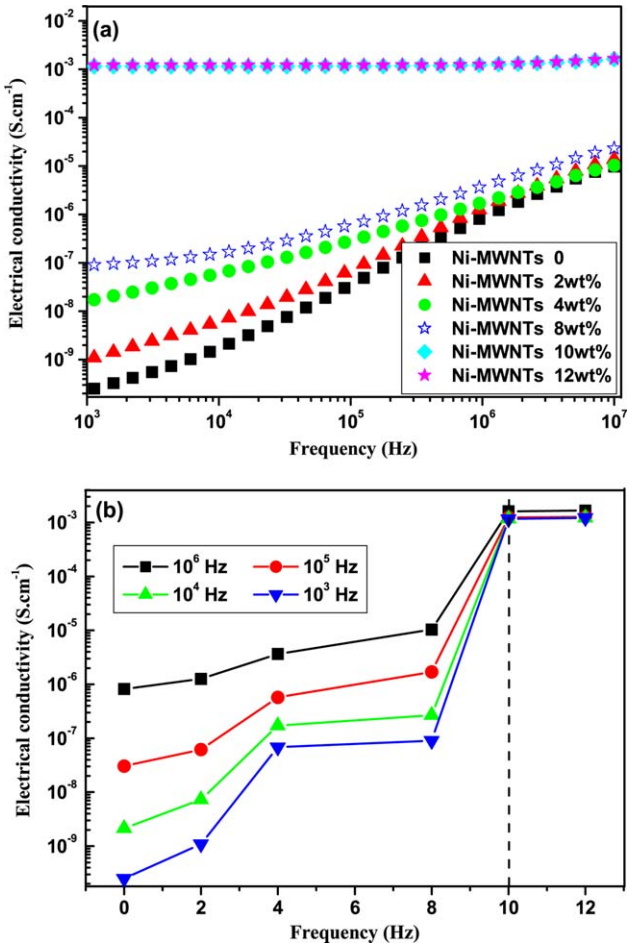

Figure 6. (a) Frequency-dependent electrical conductivity of pure PVDF and (Ni-MWNTs)/PVDF composites with various Ni-MWNTs contents and (b) electrical conductivity of pure PVDF and (Ni-MWNTs)/PVDF composites at the variation of the electric field frequency from 10^3 to 10^6 Hz. [Color figure can be viewed in the online issue, which is available at wileyonlinelibrary.com.]

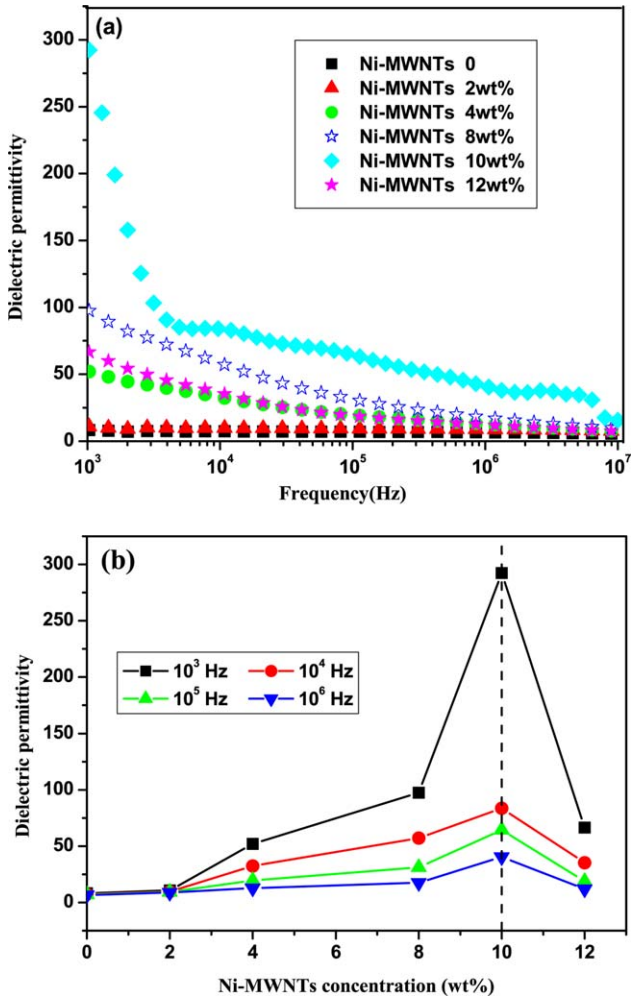

Figure 7. Dependence of the effective dielectric permittivity of composites (a) at different contents of Ni-MWNTs (0, 1, 2, 4, 8, 10, and 12 wt %) and (b) on the frequency of 10^3-10^6 Hz at room temperature, respectively. [Color figure can be viewed in the online issue, which is available at wileyonlinelibrary.com.]

MWNT contents are electrically insulating materials. In case of the composites with 4 and 8 wt % Ni-MWNTs, electrical conductivities are around $\sim10^{-8}$ and $\sim10^{-7}$ S/cm at 10^3 Hz and then they increase with increase in the frequency by reaching up to $\sim10^{-5}$ S/cm at 10^7 Hz. On the other hand, electrical conductivity of $\sim10^{-3}$ S/cm for the composites with 10 or 12 wt % Ni-MWNTs remains almost constant with the variation of the electric field frequency. Figure 6(b) indicates the change of electrical conductivity of the pure PVDF and (Ni-MWNTs)/PVDF composites at the variation of the electric field frequency from 10^3 to 10^6 Hz. The electrical conductivity is dramatically increased at a certain Ni-MWNTs content between 8 and 10 wt %. It is considered that the distance between Ni-MWNTs in the composites with a certain Ni-MWNT content between 8 and 10 wt % is close enough to form electrical conduction path via the electron hopping.

Changes of relative dielectric permittivity with the applied electric field frequency of 10^3-10^7 Hz for pure PVDF and (Ni-MWNTs)/PVDF composites with different weight fractions of Ni-MWNTs are measured at room temperature, as shown in Figure 7(a). As generally expected, the dielectric permittivity of composites would be significantly enhanced compared with that of the pure PVDF (about 8 at 10^3 Hz), and increased with weight percentage of Ni-MWNTs inclusion. Dielectric permittivity of the composite with low Ni-MWNTs content of 2 wt % is about 10 at 10^3 Hz, which remains constant irrespective of the applied electric field frequency. In case of the composites with 4 and 8 wt % Ni-MWNTs, the dielectric permittivity can reach 52 and 98 at 10^3 Hz, respectively, and decreases slowly at higher frequency range. For the composite with 10 wt % Ni-MWNTs, a high dielectric permittivity of $\sim$290 is attained at 10^3 Hz and it decreases with the increment of the applied frequency. On the other hand, for the composite with 12 wt % Ni-MWNTs content, a relatively lowered dielectric permittivity of $\sim$66 at 10^3 Hz is measured. The dielectric permittivity at 10^3, 10^4, 10^5, and 10^6 Hz of (Ni-MWNTs)/PVDF composites are compared, and the value is strongly dependent on the Ni-MWNTs content, as

shown in Figure 7(b). It is found that the dielectric permittivity reaches a maximum value substantially at 10 wt % Ni-MWNTs and then decreased for the composites with higher Ni-MWNT contents of 12 wt % at the applied electric field frequency. The large enhancement in the dielectric permittivity at low frequency is attributed to the Maxwell–Wagnar–Sillars interfacial polarization because of the different conductivity of Ni-MWNTs and PVDF.[36] For the (Ni-MWNTs)/PVDF composites, as the percolation process takes place, a sudden increase in dielectric permittivity at low frequency can be observed, which means that there are Ni-MWNTs separated by thin dielectric PVDF layers. This is in agreement with the microcapacitor model theory which will be discussed in the following section.

As we know, the dielectric permittivity is a measure of the ability of a material to be polarized by an electric field. According to the Maxwell–Wagner–Sillars effect, charges can be accumulated at the interface between two dielectric materials with different relaxation times given by τ ($=\varepsilon/\sigma$, where ε is the dielectric permittivity and σ is the electrical conductivity) when current flows across the interface between two materials.[37] Therefore, it is supposed that the high dielectric permittivity of 290 at 10^3 Hz for the composite with 10 wt % Ni-MWNTs is associated with the charge accumulation at interfacial PVDF layers wrapping individual Ni-MWNTs in the vicinity of electrical percolation threshold. As discussed above, the electrical percolation threshold of (Ni-MWNTs)/PVDF composites prepared in this study is formed at a certain concentration between 8 and 10 wt % Ni-MWNTs.

The high dielectric permittivity in percolative composites has been widely investigated and can be understood by a microcapacitor network model[16,38]: the neighboring Ni-MWNTs can be considered as electrodes and a thin layer of polymer between them acts as the dielectric, forming numerous microcapacitors in the composites. As the Ni-MWNTs content increases, not only does the number of microcapacitors increases but also the thickness of the dielectric layer decreases, resulting in high capacitance and thus high dielectric permittivity. However , Ni-MWNTs tend to form aggregates in the PVDF matrix because of the π–π interaction between individual tubes. According to the microcapacitor model, the expected number of capacitors in the composites will be reduced significantly because of the Ni-MWNTs aggregates, and thus it should be mentioned that dielectric permittivity as well as electrical percolation threshold is quite dependent on the preparation method of (Ni-MWNTs)/PVDF composites. In this study, we have prepared PVDF-based composites by ultrasonic solution mixing of nickel-functionalized MWNTs with PVDF in DMF. The mixture solution was dried in a magnetic field of 0.2T so that the nickel-functionalized MWNTs might be arranged along a certain direction to avoid the aggregation. Therefore, for the PVDF-based composites with Ni-MWNTs of 10 wt %, a high dielectric permittivity of 290 is achieved because of the maximum number of microcapacitors in the composites as well as the huge interfacial area between Ni-MWNTs and PVDF. As the Ni-MWNTs content increases to 12%, more Ni-MWNTs may tend to form aggregates in the PVDF matrix, which reduce the number of microcapacitors significantly and decreases dielectric permittivity of composites to 66.

CONCLUSIONS

(Ni-MWNTs)/PVDF composites with a high dielectric permittivity have been studied. XRD, FTIR, and DSC results demonstrate that Ni-MWNTs promote the formation of polar-phase crystals in PVDF. SEM images of (Ni-MWNTs)/PVDF composites confirm that Ni-MWNTs are dispersed uniformly in the composites by wrapped with PVDF chains. It is also found that the frequency-dependent dielectric permittivity of the composites is strongly dependent on the Ni-MWNTs content. It is characterized that the electrical percolation threshold is formed at a certain Ni-MWNTs content between 8 and 10 wt %. The dielectric permittivity of composite is as high as 290 at 10^3 Hz when the weight fraction of Ni-MWNTs is 10%, nearly 37 times that of the pure PVDF. The electrical conductivity of $\sim 10^{-3}$ S/cm for composite with 10 wt % Ni-MWNTs remains almost constant with the variation of the electric field frequency. It can be interpreted that the high dielectric permittivity and the low electrical conductivity of the composite with 10 wt % Ni-MWNTs stems from the charge accumulation at interfacial layers between PVDF chains and Ni-MWNTs disperse in the composites, and the formation of numerous "microcapacitance" structure.

ACKNOWLEDGMENTS

Contract grant sponsor: National Natural Science Foundation of China; contract grant number: 51207085. Contract grant sponsor: Innovation Key Program of Shanghai Municipal Education Commission; contract grant number: 13ZZ140. Contract grant sponsor: Natural Science Foundation of Shanghai; contract grant number: 11ZR1413500. Contract grant sponsor: Leading Academic Discipline Project of Shanghai Municipal. Education Commission; contract grant number: J51803. Contract grant sponsor: National student innovative experiment plan; Contract grant number: 012-sj-cxjh-010.

REFERENCES

1. Zhou, Z.; Mackey, M.; Carr, J.; Zhu, L.; Flandin, L.; Baer, E. *J. Polym. Sci. Part B: Polym. Phys.* **2012**, *50*(14), 993.
2. Schroeder, R.; Majewski, L. A.; Grell, M. *Adv. Mater.* **2005**, *17*, 1535.
3. Rao, Y.; Wong, C. P. *J. Appl. Polym. Sci.* **2004**, *92*, 2228.
4. Li, Z.; Fredin, L. A.; Tewari, P.; DiBenedetto, S. A.; Lanagan, M. T.; Ratner, M. A.; Marks, T. J. *Chem. Mater.* **2010**, *22*, 5154.
5. Zhang, Q. M.; Li, H. F.; Poh, M.; Xu, H. S.; Cheng, Z. Y.; Xia, F.; Huang, C. *Nature* **2002**, *419*, 284.
6. Levi, N.; Czerw, R.; Xing, S. Y.; Iyer, P.; Carroll, D. L.; *Nano. Lett.* **2004**, *4*, 1267.
7. Wang, L.; Dang, Z. M. *Appl. Phys. Lett.* **2005**, *87*, 042903.
8. Bhadra, D.; Masud, M. G.; Sarkar, S.; Sannigrahi, J.; De, S. K.; Chaudhuri, B. K. *J. Polym. Sci., Part B: Polym. Phys.* **2012**, *50*(8), 572.
9. Wang, Y.; Zhou, X.; Chen, Q.; Chu, B. J.; Zhang, Q. M. *IEEE. T. Dielect. El. In.* **2010**, *17*(4), 1036.
10. Bharti, V.; Shanthi, G.; Xua, H.; Zhang, Q. M.; Liang, K. M. *Mater. Lett.* **2001**, *47*, 107.

11. Dang, Z. M.; Wang, H. Y.; Peng, B.; Nan, C. W. *J. Electroceram.* **2008**, *21*, 381.
12. Fan, B. H.; Zha, J. W.; Wang, D. R.; Zhao, J.; Dang, Z. M. *Appl. Phys. Lett.* **2012**, *100*, 012903.
13. Xu, H. P.; Xie, H. Q.; Wu, Y. H.; Yang, D. D.; Wang, J. R. *J. Appl. Polym. Sci.* **2011**, *122*(5), 3466.
14. Xu, H. P.; Dang, Z. M.; Bing, N. C.; Wu, Y. H.; Yang, D. D. *J. Appl. Phys.* **2010**, *107*, 034105.
15. Li, Y. J.; Xu, M.; Feng, J. Q. *Appl. Phys. Lett.* **2006**, *89*, 072902.
16. Dang, Z. M.; Wang, L.; Yin, Y.; Zhang, Q.; Lei, Q. Q. *Adv. Mater.* **2007**, *19*, 852.
17. Chatterjee, J.; Nash, N.; Cottinet, P. J.; Wang, B. *J. Mater. Res.* **2012**, *27*(18), 2352.
18. Seoul, C.; Kim, Y. T.; Baek, C. K. *J. Polym. Sci. Part B: Polym. Phys.* **2003**, *41*, 1572.
19. Qi, L.; Lee, B. I.; Chen, S.; Samuels, W. D.; Exarhos, G. J. *Adv. Mater.* **2005**, *17*, 1777.
20. Kohlmeyer, R. R.; Javadi, A.; Pradhan, B.; Pilla, S.; Setyowati, K.; Chen, J.; Gong, S. Q. *J. Phys. Chem. C* **2009**, *113*, 17626.
21. Grady, B. P. *Macromol. Rapid. Commun.* **2010**, *31*, 247.
22. Kong, F. Z.; Zhang, X. B.; Xiong, W. Q. *Surf. Coat. Technol.* **2002**, *155*, 33.
23. Lovinger, A. *Macromolecules* **1982**, *15*, 40.
24. Broahurst, G. T. D. M. G.; McKinney, J. E.; Collins, R. E. *J. Appl. Phys.* **1978**, *49*, 4992.
25. Salimi, A.; Yousefi, A. *Polym. Test.* **2003**, *22*, 699.
26. Priya, L.; Jog, J. P. *J. Appl. Polym. Sci.* **2003**, *89*, 2036.
27. Tang, X. G.; Hou, M.; Ge, L.; Zou, J.; Truss, R.; Yang, W.; Yang, M. B.; Zhu, Z. H.; Bao, R. Y. *J. Appl. Polym. Sci.* **2012**, *125*, 592.
28. Huang, X. Y.; Jiang, P. K.; Kim, C.; Liu, F.; Yin, Y. *Eur. Polym. J.* **2009**, *45*, 377.
29. Newman, B. Y.; Pae, K. D.; Scheinbeim, J. I. *J. Appl. Phys.* **1979**, *50*, 6095.
30. Takahashi, Y.; Tadokoro, H. *Macromolecules* **1980**, *13*, 1316.
31. Andrew, J. S.; Clarke, D. R. *Langmuir* **2008**, *24*(3), 670.
32. Ramasundaram, S.; Yoon, S.; Kim, K. J. *Macromol. Chem. Phys.* **2009**, *210*(11), 951.
33. Kressler, J.; Schafer, R.; Thomann, R. *Appl. Spectrosc.* **1998**, *52*, 1269.
34. Damjanovic, D.; Newnham, R. E. *J. Intell. Mater. Syst. Struct.* **1992**, *3*, 190.
35. Lee, J. G.; Kim, S. H. *Macromol. Res.* **2011**, *19*, 72.
36. He, F.; Lau, S.; Chan, H. L.; Fan, *J. Adv. Mater.* **2007**, *21*, 714.
37. Tamura, R.; Lim, E.; Manaka, T.; Iwamoto, M. *J. Appl. Phys.* **2006**, *100*, 114515.
38. Huang, X. Y.; Jiang, P. K.; Xie, L. Y. *Appl. Phys. Lett.* **2009**, *95*, 242901.